

The Onset of the Madden-Julian Oscillation within an Aquaplanet Model

"EDWARD COLÓN AND JAMES LINDESAY

*The Center for the Study of Terrestrial and Extraterrestrial Atmospheres, Howard University,
Washington, D.C. 20059*

MAX SUAREZ

Laboratory for Atmospheres/Goddard Space Flight Center, Greenbelt, Maryland, 20771

ABSTRACT

A series of numerical experiments using a two-level atmospheric general circulation model (AGCM) were performed for the purpose of investigating the coupling between sea surface temperature (SST) profile and the onset of the Madden-Julian Oscillation (MJO). The AGCM was modified to run as an aquaplane with all seasonal forcing removed (Hayashi and Sumi, 1986). SST distributions based on the New Global Sea-Ice and Sea Surface Temperature (GISST) Data Set for 1903-1994 (Rayner et al., 1995) were generated then modified to vary the north-south gradient and tropical temperatures. It was found that the MJO signal did not depend on the SST temperature gradients but rather on the absolute temperature of the equatorial region, EOF analysis revealed that the SST distribution which generated the strongest MJO signal produced a periodic fluctuation in velocity potential at the 250 millibar level with a phase speed of 15 m s⁻¹ and a periodicity of 30 days which falls within the shortest limit of observed oscillations. This distribution also possessed the coolest equatorial SSTs which suggests that increased stability in the atmosphere favors the occurrence of organized MJO propagation.

1. Introduction

Large scale circulation and convection features in the tropical atmosphere have been observed to fluctuate with a certain characteristic time scales and spatial patterns. Two such global scale phenomena are the El Niño/ Southern Oscillation, which has a time scale of roughly 2 to 6 years, and the Madden-Julian Oscillation (MJO) of a corresponding oscillatory period of 30 to 60 days. The latter phenomenon was first detected by Madden and Julian (1971, 1972) using spectral analysis of daily rawinsonde data for Canton Island in the central tropical Pacific. Their observations yielded a vertically coherent tropospheric oscillation in zonal wind, pressure and temperature fields with a period of 41 to 53 days. Although they do not offer an explanation for its existence, they do observe that the oscillation is coherent through all levels of the troposphere and that it possesses characteristics of a circulation cell, which suggests that deep convection is an important driving mechanism. Over the next few years, several researchers reported the existence of a quasi-40 day cloudiness oscillations over the summer monsoon region of East Asia and India and suggested that they may be related to those found by Madden and Julian. Satellite observations of 30- to 60- day fluctuations in tropical cloudiness that tended to propagate eastward into the central Pacific also seemed to be tied to the phenomenon (Weickmann, 1983 and Weickmann et al., 1985).

A substantial body of research since then has clarified many of the fundamental characteristics associated with this oscillation. The most notable properties of are summarized as follows:

- The oscillation is characterized by global-scale tropical wind and convection anomalies, including a modulation of the Northern Hemisphere and Southern Hemisphere summer monsoon activity (Krishnamurti and Subrahmanyam, 1982)
- The oscillation is not strictly periodic, but has a preferred time scale of about 30 to 60 days.
- Convection and circulation anomalies associated with the oscillation tend to propagate eastward with time with a speed of 10-15 m/s, which is much slower than the phase speed of the equatorial Kelvin waves with the same vertical wavelength (Madden and Julian, 1972).
- in the tropics, 30-60 day zonal wind anomalies in the lower troposphere are out of phase with those in the upper troposphere and can be defined as possessing baroclinic structure (Murakami and Nakazawa, 1985).
- Coherent fluctuations between extratropical circulation anomalies and the tropical 30-60 day oscillations may exist, indicating possible tropical midlatitude interactions in the above time scale (Weickmann et al., 1985).

The origin of the **MJO** has remained an enigma since its initial detection. In this study we will look at three explanations: **wave-CISK** mechanism (**Lau and Peng, 1987; Hendon, 1988**), evaporation-wind feedback (**Emmanuel, 1987; Neelin, Held and Cook, 1987**) and the super cloud cluster forcing mechanism (**Chao and Lin, 1993; Chao, 1995**).

2. Theory

Much of tropical **meteorology** involves the collective interaction of large-scale circulation dynamics and **cumulus** convection. The candidate most likely responsible for this interaction is conditional instability of the second kind (**CISK**) (**Charney and Eliassen, 1964**). This mechanism is characterized by a low-level convergence field associated with a large-scale meteorological system that lifts surface air to a given height where cumulonimbus convection occurs. The latent heat released by this convection forces a large-scale motion whose low-level convergence in turn helps maintain the convection. Underlying **all CISK** models is the assumption that deep cumulus convection will not, by **itself**, maintain the low level convergence necessary for the maintenance of clouds. Consequently, some large-scale, low-level convergence is necessary. Preliminary studies of **CISK** generating mechanisms pointed to the possibility of **Ekman** pumping as providing the **necessary** convergence (**Charney and Eliassen, 1964**). However, near the equator the term associated with momentum flux divergence vanishes, making **Ekman** pumping an unlikely candidate for providing the necessary forcing. It is now generally accepted that **equatorially** trapped internal **waves**(**gravity, Kelvin, mixed gravity-Rossby, and Rossby**), which are highly convergent, can produce **CISK** without the need of **Ekman** pumping (**Lindzen, 1974**).

Hendon (1988), used a two level model and a **CISK-type** cumulus heating scheme to obtain a reasonable simulation of the **MJO** and identified its structure as that of a nonlinearly coupled **Rossby-Kelvin** mode. It was found that an east ward propagating **CISK** mode, consisting of a **Rossby** wave component to the west and a Kelvin wave component to the east, is in agreement with observations. The **Rossby** component is **continuously** generated as the disturbance moves eastward. Consequently, we should be able to observe a meridional wind perturbation accompanying the eastward moving **oscillation; this, in fact**, has been **observed** (**Madden, 1986**) and **modelled** (**Hayashi and Sumi, 1986**). This **CISK** mode is similar in structure to the quasi-steady response (**Gill, 1980**) to slow eastward moving **diabatic** forcing. There is a pronounced east-west asymmetry in the **equatorial** region. Kelvin waves **carry** the information rapidly **eastward**, thereby creating **easterly** low-level winds in that region. These winds provide inflow to the **region** of heating and subsequently initiate a Walker-type circulation with rising over the source region and sinking to the east. Additionally, heating would generate **Rossby** waves which would carry information westward.

We can gain a better understanding of the coupled **Rossby-Kelvin** mode by **examining** the **equatorially** trapped **free** oscillations using the beta-plane approximation (**Hendon, 1988**) from which the following arguments have been derived. **Assuming** that there is no initial meridional forcing in the tropics, we can express the horizontal momentum equations as

$$\frac{\partial u}{\partial t} - \beta y v = -\frac{\partial \Phi}{\partial x}, \quad (1)$$

$$\beta y u = -\frac{\partial \Phi}{\partial y}, \quad (2)$$

$$\frac{\partial \Phi}{\partial t} + c^2 (\nabla \cdot U) = K^2 (\nabla \cdot U) \quad (3)$$

where $\beta = 2\Omega/R$, u is the perturbation **zonal** wind, v is the perturbation meridional **wind**, Φ is the **geopotential**, c is the velocity of propagation, U is the sum over perturbations in **zonal** and meridional wind, and K is cumulus heating factor. For this particular model $c^2 (=gH) = (p/p_0)^{R/C_p} C_p \theta_0$ and $K^2 = (p/p_0)^{R/C_p} C_p Q'$ where θ is the potential **temperature** and Q' is the ratio of combined steady **diabatic** heating and cumulus heating to $\nabla \cdot U$. The **equatorially** trapped wave solutions (**Holton, 1992**) can be derived **from** Eqs. (1), (2), and (3) so that

$$\begin{pmatrix} u \\ v \\ \Phi \end{pmatrix} = \begin{pmatrix} u(y) \\ v(y) \\ \Phi(y) \end{pmatrix} H_n(y) \exp[i(kx - \omega t)], \quad (4)$$

and the dispersion relation is given by

$$\omega = -\frac{kC}{2n + 1} [1 - (K/c)^2]^{1/2}, \quad (5)$$

where n is the meridional mode number, $H_n(y)$ represents the **Hermite** polynomial of degree n , and k is the **zonal wavenumber**. The Kelvin wave dispersion is obtained for $n = -1$ and $n = 1$ yields the most prominent **Rossby** wave.

For $K^2 = 0$ (no cumulus heating) the solutions yield a dry Kelvin wave which propagates eastward at $c = ((p/p_0)^{C_p} C_p \theta)^{1/2} \approx 60 \text{ m s}^{-1}$ which is roughly three times faster than the induced $n = 1$ **Rossby** wave. For $0 < K < c$ (stable cumulus heating), moisture modified waves are slowed by a factor of

$$[1 - (K/c)^2]^{1/2} = [1 - (Q'/\theta)]^{1/2}. \quad (6)$$

It is obvious that eastward propagating Kelvin waves can be reduced to any phase speed with the appropriate choice of Q' . For $K^2 > c^2$ (unstable condition), the dispersion relation takes the form $i\omega$ where ω is defined by Eq. (5). In this case, **all** waves are stationary and increasing in amplitude due to the fact that they possess imaginary phase speeds. It is possible that a propagating coupled mode may exist in the linear model when $\theta < Q'$ which implies that the individual **Rossby** and Kelvin modes will have **imaginary** phase speed. However, a horizontally coupled propagating mode could exist in the presence of positive cumulus heating.

An alternative **mechanism** for **MJO** generation has been proposed by Emmanuel (1987), and Neelin, Held, and Cook (1987) that acts through a feedback between evaporation and surface winds. The major limitation of evaporation-wind (E-W) feedback as a modulating mechanism for Kelvin wave propagation is that it assumes that lower tropospheric easterly equatorial flow is a **mandatory** basic state when in fact observations have clearly revealed westerlies in the Indian Ocean (Wang, 1988). Additionally, Chao (1994, 1995) has linked the development of the **MJO** to the cloud cluster **teleinduction** mechanism. Satellite observations have shown that convective regions associated with this oscillation consist of one or more super cloud clusters and within each of them individual cloud clusters arise, move westward, and then decay within 2 to 3 days. New cloud clusters appear to the east of the existing cloud clusters. The reason that the eastern side of an existing cloud cluster is more favorable than the western side for the new cloud cluster formation has to do with basic flow in the boundary layer being easterly which is also strengthened by the circulation induced by the existing cloud cluster. In other words, the east side provides the primary moisture supply. Once the new cloud cluster emerges, it competes for moisture supply with the existing cloud cluster. The existing cloud cluster weakens as it propagates westward into the area of depleted moisture which is consumed by the newly developed cloud cluster. Successive generation of new cloud clusters in the east and the subsequent decay of existing ones give rise to an eastward moving envelope, which is the super cloud cluster associated with the **MJO**.

3. Model

A two-level general circulation model (Zephyr) based on an older primitive equations model developed by Held and Suarez (1978) is employed to examine **MJO** development and propagation. It utilizes **DYCORE**, the standard C-grid ($4^\circ \times 50$, dynamical core used by NASA/Goddard **GCMs**). Zephyr is characterized by simple cumulus **parameterization**, and full a hydrologic cycle. In a manner similar to Hayashi and Sumi (1986), Zephyr is modified to run as an **aquaplanet** in which earth's surface is covered by a uniform global ocean. This change can be made since the oscillation is primarily dependent on the moisture content of the tropical region and the **oscillatory** structure of the **phenomenum** is more readily observable without the effects of intervening land-masses. Zephyr is an atmosphere-only model (**AGCM**) so that a fixed **zonally** symmetric sea surface temperature (SST) distribution is employed. The temperature profile is based on the New Global Sea-Ice and Sea Surface Temperature (**GISST**) Data Set for 1903-1994 (Rayner et al., 1995). **GISST** is composed of monthly averaged **SSTs** which have been resolved using **eigenvector** (EOF) reconstruction methods. Data resolution is $1^\circ \times 10$ for absolute SST readings back to 1982, and 20×20 for anomalous **SSTs** taken back to 1949. Prior to 1949

anomalous SSTs have a resolution of $5^{\circ} \times 5''$. The advent of remote sensing and systematic data collection has allowed for better grid resolution since 1982.

A $4^{\circ} \times 50$ zonal average was taken for GISST data set so that it could be utilized by Zephyr. A slightly asymmetric SST profile resulted between the northern and southern hemispheres. Since we wanted to achieve a fairly realistic aquaplanet profile, it was decided to “flip” the southern hemisphere SST readings into the northern hemisphere deleting any anomalous effects due to land-masses and thus providing a truly zonally symmetric SST profile with a maximum temperature of 28.6°C at the equator and a minimum of -2°C at the poles. Since Zephyr was originally intended to examine interannual phenomena dependent on seasonal fluctuations, we had to modify several subroutines in order to observe daily perturbations with the seasonal variability essentially “turned off”. Additionally, Topography was flattened in order to remove any orographic forcings and albedo was set at 0.07 which corresponds to that of ocean water. Horizontal diffusion is handled by means of an eighth order Shapiro filter used to curtail nonlinear computational instability initiated by the cascade of variance to short horizontal scales.

4. Preliminary Results

An initial experiment was conducted with the goal of obtaining a realistic simulation of MJO-like propagations within the equatorial region of the model. In order to investigate the connection between SST profiles and the MJO, five different distribution with incrementally decreasing pole to equator temperatures were tested. The first run was performed using the original GISST profile. Once the model climatology was deemed acceptable, analysis was made of the 250- and 750-millibar level zonal wind (u), precipitation(p), latent heat flux (FL), velocity potential (χ) and divergence of wind velocity ($\nabla \cdot \mathbf{U}$). Hovmöller diagrams of u, χ , and χ revealed little in terms of a stable eastward propagating oscillatory signal with the characteristic 30-60 day period. However, a weakly defined easterly flow was observed at the equator of order 10 m s^{-1} . The initial GISST profile was modified so that the SSTs were linearly decremented in the tropics yet held constant at the poles. All other parameterizations were held constant and each model was run for 365 days plus an additional 100 days spin up time. Five meridional temperature profiles were examined starting with the initial pole to equator distribution ranging from -2°C to 28.6°C , and ending with a distribution that ranged from -2°C to 23.6°C . Of the five distributions, the -2°C to 23.6°C profile yielded the strongest MJO signal. The following Hovmöller diagrams and figures are for the this case. Figures 1 and 2 reveal the periodic structure of the MJO phenomenon.

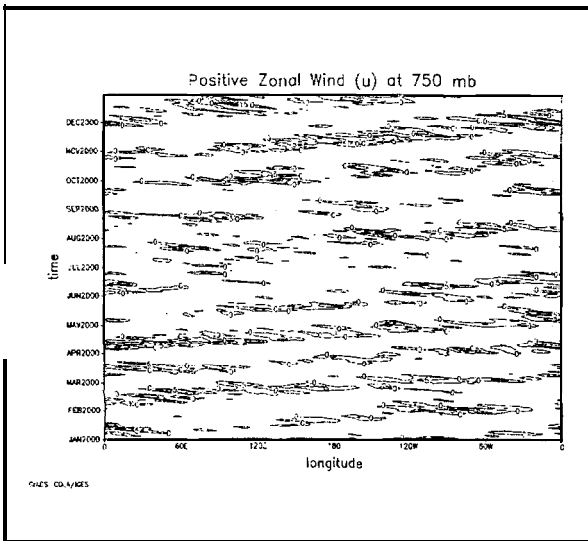


Figure 1. Hovmöller diagram of zonal wind at 750 mb. ($0-5 \text{ m s}^{-1}$ contour)

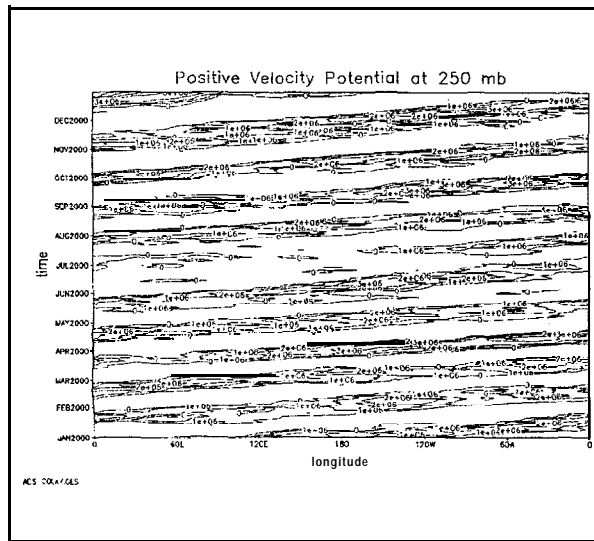


Figure 2. Hovmöller diagram of χ_{250} .

Based on the relatively systematic time evolution of the 30-60 day χ_{250} anomalies, we elected to use an empirical orthogonal function (EOF) analysis of this data to determine the time variation and phase of the oscillation. Figure 3 below depicts the first two eigenvectors (spatial patterns), while figure 4 illustrates the principal component (time series). It is interesting to note that first two principal components describe 40% and 38% of the χ_{250} 30-60 day variance

respectively. Additionally, there is a 900 phase shift **between the first and second eigenvalues** and principal components. A period of **roughly 30 days** is observed in the time series which entails a **MJO propagation velocity of 15 m S-l**.

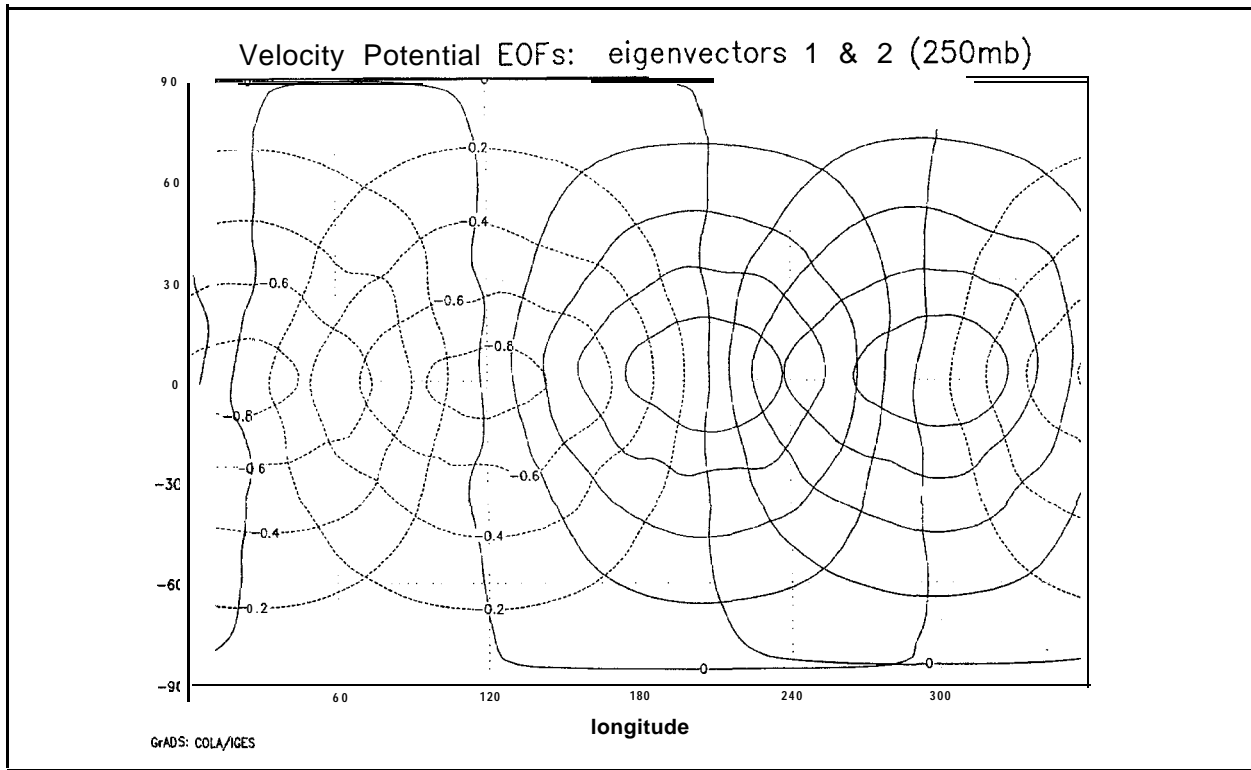


Figure 3. First and second **eigenvectors** of χ_{250} . Solid line designates positive **EOFS**, dashed lines designates negative **EOFS**. Contour internal is set at 0.2.

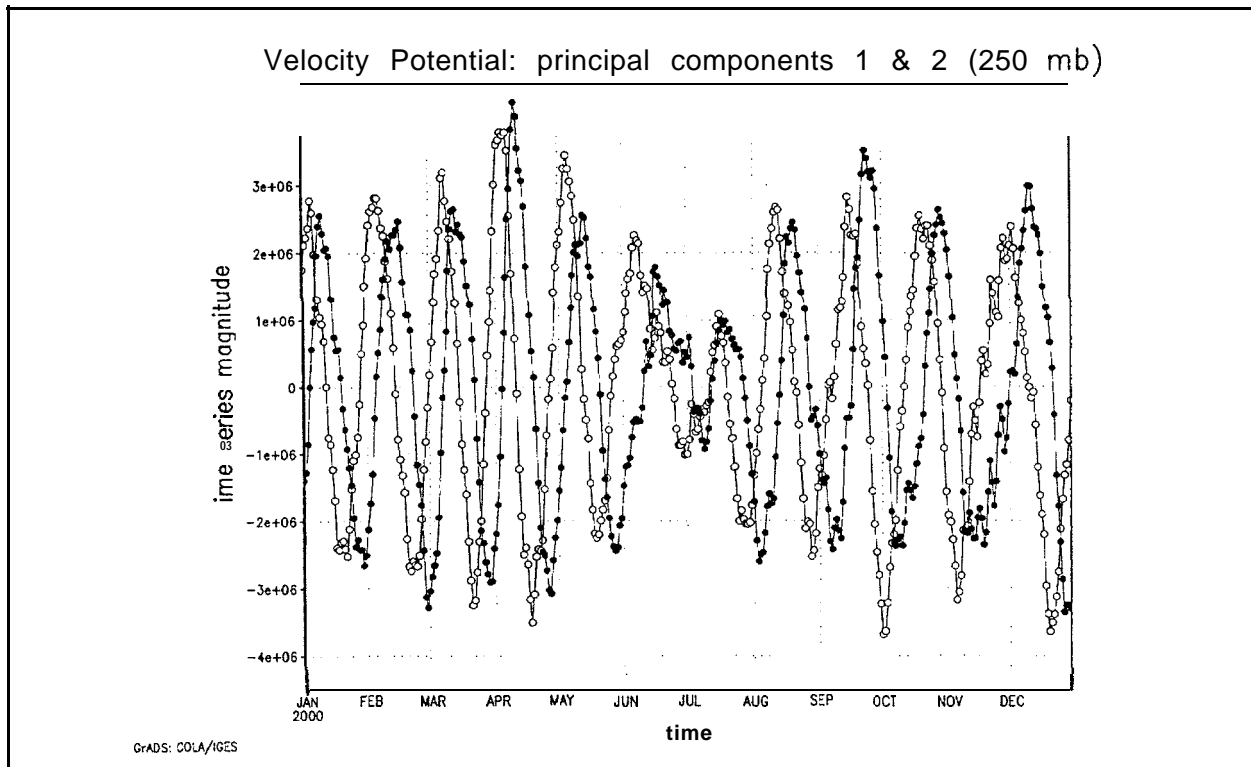


Figure 4. First (hollow circle) and second (solid circle) principal components of the MJO derived from χ_{250} .

4. Conclusion

The fact that the case that yielded the strongest **MJO** signal possessed the smallest temperature gradient between the pole and equator as well as the lowest equatorial temperatures raised the question as to which of these effects were responsible for the enhanced oscillation. A **final** experiment was performed in which the weakest gradient profile was shifted upward until temperatures at the equator corresponded to those of the original **GISST** distribution. It was found that the simulated fields matched those produced by the original **GISST SSTs** pointing to the possibility that for stable conditions, only damped moist Kelvin waves are generated. These waves are quickly dissipated for lack of a driving mechanism. Because the **adiabatic** heating effectively reduces the static stability, and hence the rate of temperature change associated with vertical motions, moist Kelvin waves propagate at a reduced phase speed compared to dry waves—the stronger the heating, the slower the propagation (**Bladé and Hartmann, 1993**). This scenario would explain the weakened signal and slower phase speeds attained by SST profiles possessing warmer equatorial temperatures. Future research will examine transitional profiles for which dry Kelvin waves will be generated as well as looking **exclusively** at meridional wind velocity in order to gain a better understanding of the **Rossby** wave component associated with the oscillation. Additionally, longer three year runs will be performed in order to compile a larger statistical sampling of the **MJO** generated signals.

Acknowledgements. We would like to thank Howard University's Center for the study of Terrestrial and Extraterrestrial Atmospheres and the NASA Goddard Space Flight Center **Laboratory** for Atmospheres for support and technical assistance.

REFERENCES

- Bladé, I. and D. L. Hartmann, 1993:** Tropical intraseasonal oscillations in a simple nonlinear model. *J. Atmos. Sci.*, **50**, 2922-2939.
- Chao, W. C. and Lin, S-J, 1994:** Tropical intraseasonal oscillations, super cloud clusters, and cumulus convection schemes. *J. Atmos. Sci.*, **51**, 1282-1297.
- , **1995:** A critique of wave-CISK as an explanation for the 40-50 day tropical intraseasonal oscillation. *J. Meteor. Soc. Japan*, **48**, 677-683.
- Charney, J. G. and A. Eliassen, 1964:** On growth of the hurricane depression. *J. Atmos. Sci.*, **21**, 68-75.
- Emmanuel, K. A., 1987:** An air-sea interaction model of intraseasonal oscillations in the tropics. *J. Atmos. Sci.*, **44**, 2324-2340.
- Gill, A. E., 1980:** Some simple solutions for heat induced tropical circulation. *Quart. J. Roy. Meteor. Soc.*, **106**, 447-463.
- Hyashi, Y.-Y., and A. Sumi, 1986:** The 30-40 day oscillations simulated in an "aqua planet" model. *J. Meteor. Soc. Japan*, **64**, 451-466.
- Held, I. M. and M. J. Suarez, 1978:** A two level primitive equation model designed for climatic sensitivity experiments. *J. Atmos. Sci.*, **35**, 206-229.
- Hendon, H. H., 1988:** A simple model of the 40-50 day oscillation. *J. Atmos. Sci.*, **45**, 569-584.
- Holton, J. R., 1992:** An introduction to dynamic meteorology. Academic Press, 392 pp.
- Krishnamurti, T. N. and D. Subrahmanyam, 1982:** The 30-50 day mode at 850 mb during MONEX. *J. Atmos. Sci.*, **39**, 2088-2095.
- Lau, K. M. and L. Peng, 1987:** Origin of low-frequency (intraseasonal) oscillations in the tropical atmosphere. Part I basic theory. *J. Atmos. Sci.*, **47**, 950-972.
- Lindzen, R. S., 1974:** Wave-CISK in the tropics. *J. Atmos. Sci.*, **31**, 156-179.
- Madden, R. A. and P. R. Julian, 1971:** Detection of a 40-50 day oscillation in the zonal wind in the tropical Pacific. *J. Atmos. Sci.*, **28**, 702-708.
- , and ———, 1972: Description of global-scale circulation cells in the tropics with a 40-50 day period. *J. Atmos. Sci.*, **29**, 1109-1123.
- , 1986: Seasonal variations of the 40-50 day oscillation in the tropics. *J. Atmos. Sci.*, **43**, 3138-3158.
- Murakami, T., and T. Nakazawa, 1985:** Tropical 40-50 day oscillations during the 1979 northern hemisphere summer. *J. Atmos. Sci.*, **42**, 1107-1122.
- Neelin, J. D., I. M. Held, and K. H. Cook, 1987:** Evaporation-wind feedback and low frequency variability in the tropical atmosphere. *J. Atmos. Sci.*, **44**, 2341-2348.
- Rayner, N. A. et al, 1995:** A New Global Sea-Ice and Sea Surface Temperature (**GISST**) Data Set for 1903-1994 for forcing Climate Models, **Wadati** Conference on Global Climate Change and the Polar Climate, Tsukuba, Japan.
- Weickmann, K. M., 1983:** Intraseasonal circulation and outgoing longwave radiation modes during Northern Hemisphere winter. *Mon. Wea Rev.*, **111**, 1838-1858,
- , G. R. Lussky and J. E. Kutzbach, 1985: Intraseasonal (30-60 day) fluctuations of outgoing longwave radiation and 250 mb streamfunction during northern winter, *Mon. Wea Rev.*, **113**, 941-961.